Journal of King Saud University – Computer and Information Sciences 34 (2022) 72–85

Contents lists available at ScienceDirect

Journal of King Saud University – Computer and Information Sciences

journal homepage: www.sciencedirect.com

Zoom based image super-resolution using DCT with LBP as characteristic model

Meera Doshi [a,*], Prakash Gajjar [b], Ashish Kothari [a]

[a] Atmiya Institute of Technology and Science, Rajkot, India
[b] Government Polytechnic for Girls, Surat, India

ARTICLE INFO

Article history:
Received 12 March 2018
Revised 7 October 2018
Accepted 8 October 2018
Available online 13 October 2018

Keywords:
Discrete cosine transform (DCT)
Learning-based approach
Local binary pattern (LBP)
Mean Squared Error (MSE)
Peak signal to noise ratio (PSNR)
Super-resolution (SR)
Structural Similarity Index (SSIM)

ABSTRACT

The prime intention of super-resolution (SR) technique is to restore the high-resolution images from one or more low-resolution (LR) images. These images are captured from the same scene with different acquisition systems with different resolution. Because these acquisition systems, images are suffered for an ill-posed problem with low visualization and picture information. Therefore, in this paper, the zoom-based super-resolution approach is proposed for super-resolution of low resolute images which are acquired from different camera zoom-lens. In this approach, three LR images of the same static scene which are acquired using three distinct zoom factors are used. Learning-based SR technique is used to enhance the spatial resolution of these LR images. The training dataset comprises three sets of captured images which are LR images, an enhanced version of LR images-HR1 and enhanced version of HR1 images-HR2. High-frequency details of the super-resolute image are learned in form of the discrete cosine transform (DCT) coefficients of HR training images. Finally, the super-resolved versions of LR observations, captured at different zoom-factors, are combined. The experimental results show that this proposed approach can be applied to various types of natural images in grayscale as well as color. The experimental results also show that this proposed approach performs better than existing approaches.

1. Introduction

"One picture is worth a thousand words." This proverb correctly expresses the amount of information contained in a picture. Pictures are the most effective form of information representation for mass communication. The images with superior qualities are needed in almost all imaging applications. The high-quality images that provide more detailed information are crucial in applications such as clinical diagnosis, biometrics, industrial inspection, surveillance, remote sensing, and machine vision etc. High-resolution images provide better analysis, classification, and interpretation. Even if using advanced fabrication methods for imaging sensors, it is required to compromise the available signal to noise ratio (SNR), pixel size and spatial resolution. Thus, it is essential to employ techniques of signal processing for image enhancement, which increase the image resolution. The super-resolution (SR) is such signal processing techniques or algorithm in which high spatial resolution (HR) image is reconstructed from one or more low resolution (LR) images. SR techniques are classified as (Tian and Ma, 2011; Park et al., 2003) (i) Frequency- Domain Approach (Ji and Fermüller, 2009; Chappalli and Bose, 2005; El-Khamy et al., 2005), (ii) Interpolation based approach (Aftab et al., 2008; Suresh and Rajagopalan, 2007), (iii) Regularization based Approach (Belekos et al., 2010; Shen et al., 2007; Jung and Ju, 2013; Zibetti et al., 2011; Vicente et al., 2016), and (iv) Learning-based Approach (Hertzmann et al., 2001; Wang et al., 2010; Kim and Kwon, 2010; Mu et al., 2011; Kim and Kwon, 2008). In the first three techniques, the super-resolute image is obtained from one or more LR images. While in the fourth technique, the super-resolute image is obtained from image dataset. In learning-based SR method, high-frequency information is learned from the dataset comprising of LR-HR pairs of training images.

Gajjar et al. (Gajjar and Joshi, 2008) used recorded image dataset which is made up of LR images and their equivalent HR images. In this approach, the HR test image is estimated by learning of Dis-

* Corresponding author.
E-mail addresses: meera.doshi82@gmail.com (M. Doshi), gajjar_prakashchandra@gtu.edu.in (P. Gajjar).
Peer review under responsibility of King Saud University.

Production and hosting by Elsevier

https://doi.org/10.1016/j.jksuci.2018.10.005
1319-1578/

crete Wavelet Transform (DWT) coefficients of LR images. The restriction of this approach is its incapability to retain complex edges and fine details available in images. Pithadia et al. (2012) proposed a learning-based approach using DCT. In this approach, high-frequency details of HR image are learned from DCT coefficients of LR images. The limitation of this approach is that it is used only one LR image for reconstruction of the HR image.

To overcome the limitation of these existing approaches, the new super-resolution method is proposed in this paper. In this approach, the sequence of images of static scenes is recorded at distinct zoom factors. The resolution of the resultant image of the whole scene is equivalent to the most zoomed resolution of acquired images in this approach. In this approach, three LR images with different zooming factors are used for testing purpose. In learning-based approach, training dataset which are comprised images at three different resolutions. These comprised images are LR images, an enhanced version of LR images-HR1 and enhanced version of HR1 images-HR2.

This proposed approach overcomes some limitations of Kalariya scheme (Kalariya et al., 2015) which is DCT based learning approach. The limitation of Kalariya scheme is that lack of ability to learn edges and texture quality of the image. The reason behind this limitation is during the learning of high-frequency details, they compare discrete cosine transform coefficients at each single pixel location only and do not consider the geometric structure surrounding to that pixel. While in the proposed approach, high-frequency details are learned from LR and HR image pairs of training dataset with local binary pattern coding. So, detail texture of the image, as well as intrinsic edges information, can be retrieved, which results in improved SR image. The comparison of results is done with the standard Bicubic interpolation method and Kalariya scheme (Kalariya et al., 2015).

The rest of paper is organized as follows: in Section 2, zoom based learning approach is described. Section 3 gives information on proposed approach for image super-resolution. Section 4 gives a proposed approach for super-resolution of color images. The results and discussion for the performance of the proposed scheme for various types of images are given in Section 5. Finally, the conclusion is given in Section 6.

2. Zoom based learning approach

Initially, the concept of learning-based image super-resolution via zoomed images was introduced by Joshi et al. (Joshi et al., 2005) and further developed by Gajjar et al. (Gajjar et al.,2006; Gajjar and Joshi,2010). They presented that the amount of aliasing in the image varies with zooming. So that, fewer numbers of image pixels are used in the acquisition of the zoomed image. But problem arises in this method is that it captured a larger area than acquired zoomed image. Thus, sampling rate increase and aliasing effect decrease with increment in zoom factor. Simultaneously level of blurring also changes with the level of zooming. So, the factor of zoom can be used as a mark to obtain high-resolution image a sign to generate high-resolution images of the least zoomed scene. $\{S'_n\}_{n=1}^{r}$ is the sequence of r images with a size of M × M pixels of the static scene captured at distinct camera zoom factor. Zoom factor of these images is in increasing order means S'_1 is the least zoomed image and S'_3 be the most zoomed image where $r = 3$. It is assumed that the zoom factor is known as successive observations. The correlation between these LR images and its corresponding HR images is shown in Fig. 1 for $r = 3$.

The proposed zoom-based technique is shown in Fig. 2. The observed scene is recorded at three distinct camera zooms in this approach. There are three images represented as Least Zoom (LZ) imageS'_1, Zoom (Z) image S'_2 and Most Zoom (MZ) imageS'_3. The size ofS'_1 toS'_3 is M × M. S'_1 image is represented by a few numbers of pixels. It can cover the whole scene but it has the minimum resolution. But in comparison to S'_1 image, S'_2 image covers a lesser part of the scene but it has a good resolution. Compare to both, S'_3 image represents only a small part of the scene with finest resolution. Using proposed SR technique, first S'_1 image is magnified by a factor of four. It is called as LZ_Enhanced image and denoted as a LZ_E image. Likewise, with the proposed SR technique, Z-S'_2 image is magnified by a factor of two. It is called as Z_Enhanced image and denoted as a Z_E image. Fig. 3 shows a combination of LZ_E, Z_E and MZ_S'_3 images. The resultant SR image Z′ is most zoomed observed image with higher resolution compared to combined images.

3. Proposed approach

Super-resolution is an ill-posed inverse problem in which the data is recovered from one or more degraded low-resolution images. This proposed approach is described to resolve this kind of issue. In this section, proposed super-resolution approach using discrete cosine transform (DCT) and local binary pattern (LBP) modelling is described. Fig. 4 shows the block diagram of proposed approach. Here, first, the training dataset comprising three sets of images which are recorded at three different zoom factors of a camera, 1×, 2× and 4×. The SR technique can be subdivided into the four steps which are described in next paragraph.

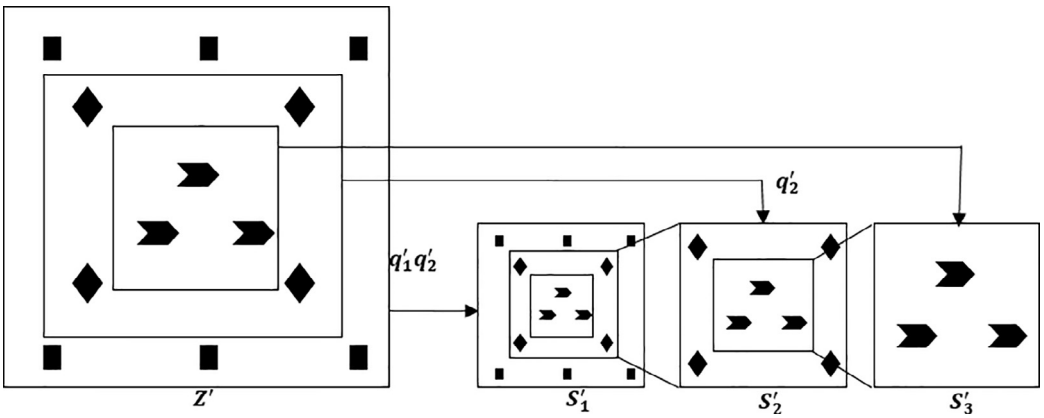

Fig. 1. Representation of the formal correlation amongst the LR observationsS'_1, S'_2 and S'_3 and super-resolute imageZ'. S'_1-least zoomed image and S'_3-most zoomed image. q'_1 And q'_2 are decimation factor.

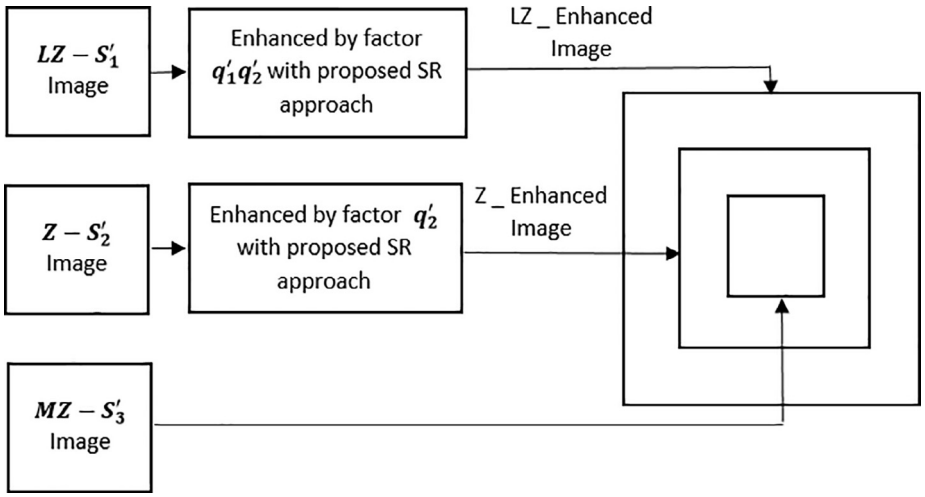

Fig. 2. Block diagram of proposed Zoom Based Approach.

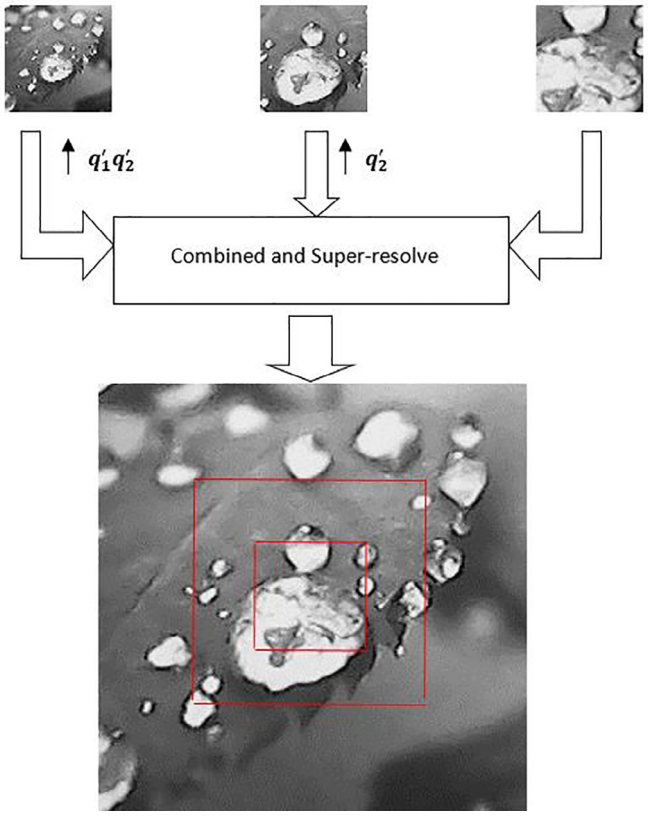

Fig. 3. Illustration of the three LR records at different zoom factor Upper row shows three LR observations at different zoom factors. The lower row shows constructed a super-resolute image. The square represents area covered by the first and second LR observation after super-resolution of individual observation.

In the first step, the LR test image and LR training images recorded at 1x zoom factor are up-sampled by the factor of 2 using the Bicubic method of interpolation. In the second step, two tasks are performed. The first task is block-based discrete cosine transform of the upsampled LR test image and HR images. The second task is designing LBP model of the upsampled Test image and upsampled LR training images. The next step is of searching the training images that have similar features to the test image using LBP modelling of images. Succeeding step comprising discrete cosine transform based learning of high-frequency coefficients. Finally, super-resolute test image of size 2× is obtained by taking inverse discrete cosine transform on outcome image of the fourth step. These all steps are repeated on test image of size 2× to obtain a super-resolute image of size 4×. The succeeding section contains the more detailed explanation of the proposed approach.

3.1. Discrete cosine transform

In the field of image processing, the Discrete Cosine Transform (DCT) is the famous technique of analysis (Rhee and Kang, 1999; Parmar and Scholar, 2014; Dabbaghchian et al., 2010). The drawback of two-dimension wavelet is that it is unable to capture directional information of image. The DCT based learning approach can capture the intrinsic geometrical structures of natural images. Thus, in proposed learning algorithm, DCT based learning approach searches the fine details of the super-resolute image from the database on LR-HR images and recovers the geometrical structures of natural image. When DCT is applied to any image than DCT coefficients give pixel intensity of the image. The DC coefficients have low frequencies while AC coefficients have high frequencies. This technical characteristic of DCT can be employed to retrieve certain important features of an image. Suppose the size of the test image is M × M. The size of the LR training image is M × M and HR training image is 2 M × 2 M. The test image and LR training images are upsized to 2 M × 2 M as shown in Fig. 5.

Then test image and HR training images are segmented into 8 × 8 pixels patches and DCT is applied onto each of the 8 × 8 pixels patches of the test image and HR Training images of size 2 M × 2 M. Thus, all HR training images and test images are represented in matrices of DCT coefficients. At the position (0,0) the coefficient shows the DC level of the images.

3.2. LBP modelling of images

In this step, the features of the image are modelled using local binary pattern operator. Image characteristics such as edges, curves, corners, and junctions can be represented more effectively by the surrounding local information of the pixel under consideration. The concept of LBP was initially suggested by Ojala et al. (2002) for classifying texture. After that original LBP and its variations are suggested in different application such as face recognition (Ahonen et al., 2006), object detection (Pereira et al., 2010) etc. LBP is more efficient to identify variations in the local structure of the image than traditional structural models for texture analysis. To

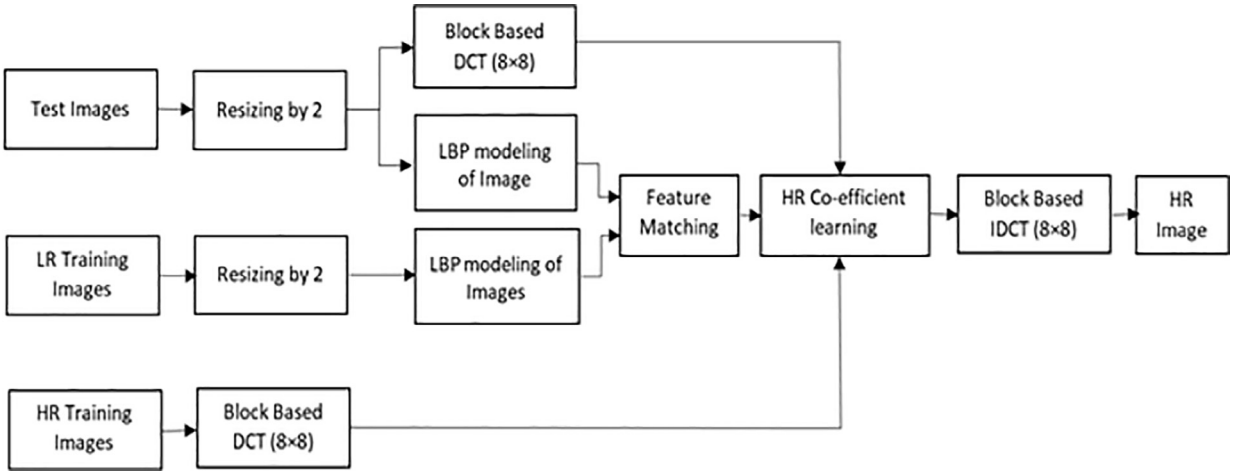

Fig. 4. Block Diagram of Proposed Super-Resolution Approach.

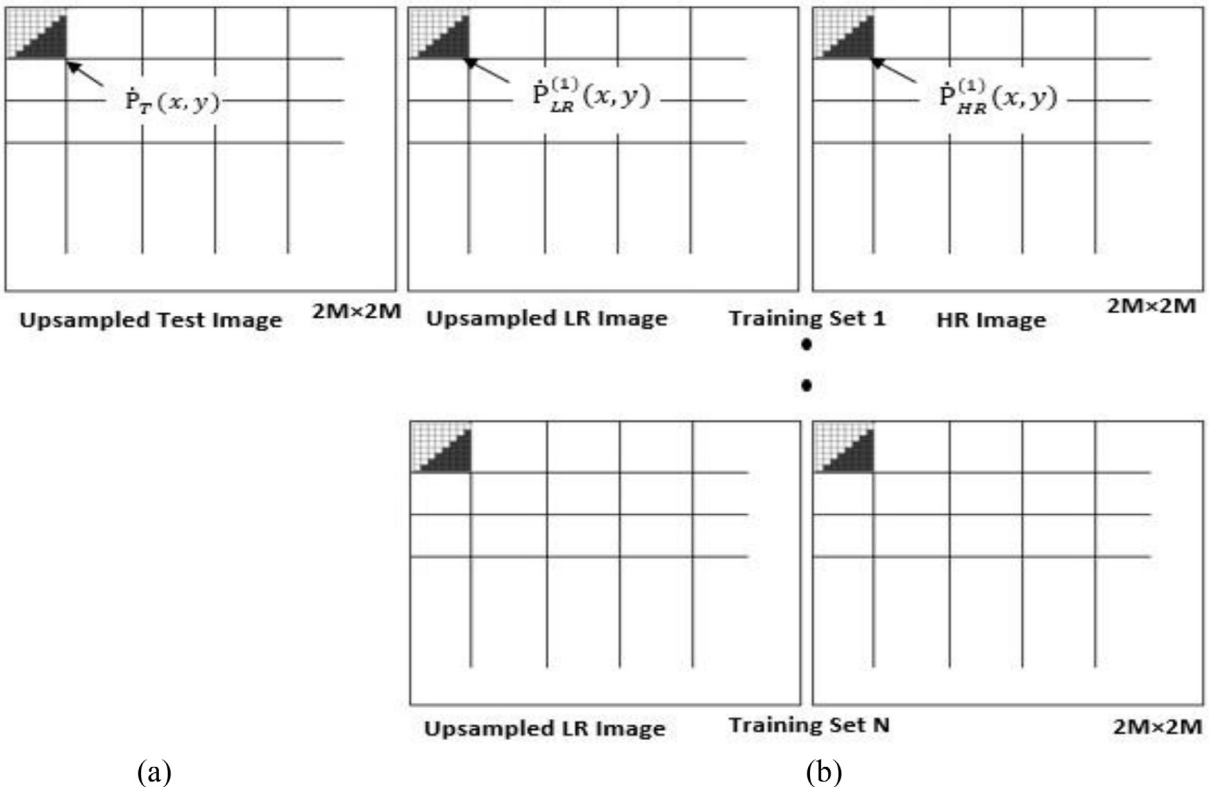

Fig. 5. Learning DCT coefficients from a database of sets of LR-HR images. (a) Upsampled test image and (b) sets of upsampled LR images and HR images for different scenes. DCT coefficients for the shaded locations in the upsampled test image are copied from corresponding locations of the best matching HR image.

design LBP code of pixel, the intensity of image pixel is compared with its all neighboring pixels. LBP code of the pixel at the position (i, j) can be found using below equation (1):

$$I(x,y) = \sum_{n=1}^{n=7} f(D_n - I) \cdot 2^n \tag{1}$$

where $f(x) = \begin{cases} 1, x > \theta \\ 0, x \leqslant \theta \end{cases}$, θ is a threshold value, $I(x, y)$ is a pixel intensity at location (x, y) and D_n is a pixel intensity of all neighboring pixels.

The LBP coding method used in proposed approach is given in Fig. 6. Different types of LBP codes are given in Fig. 7. Initially,

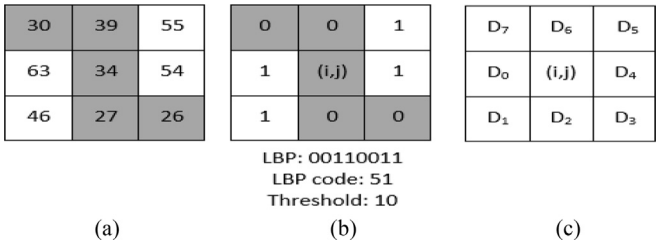

Fig. 6. (a) An image patch of size 3 × 3 (b) its binary pattern (c) its LBP coding.

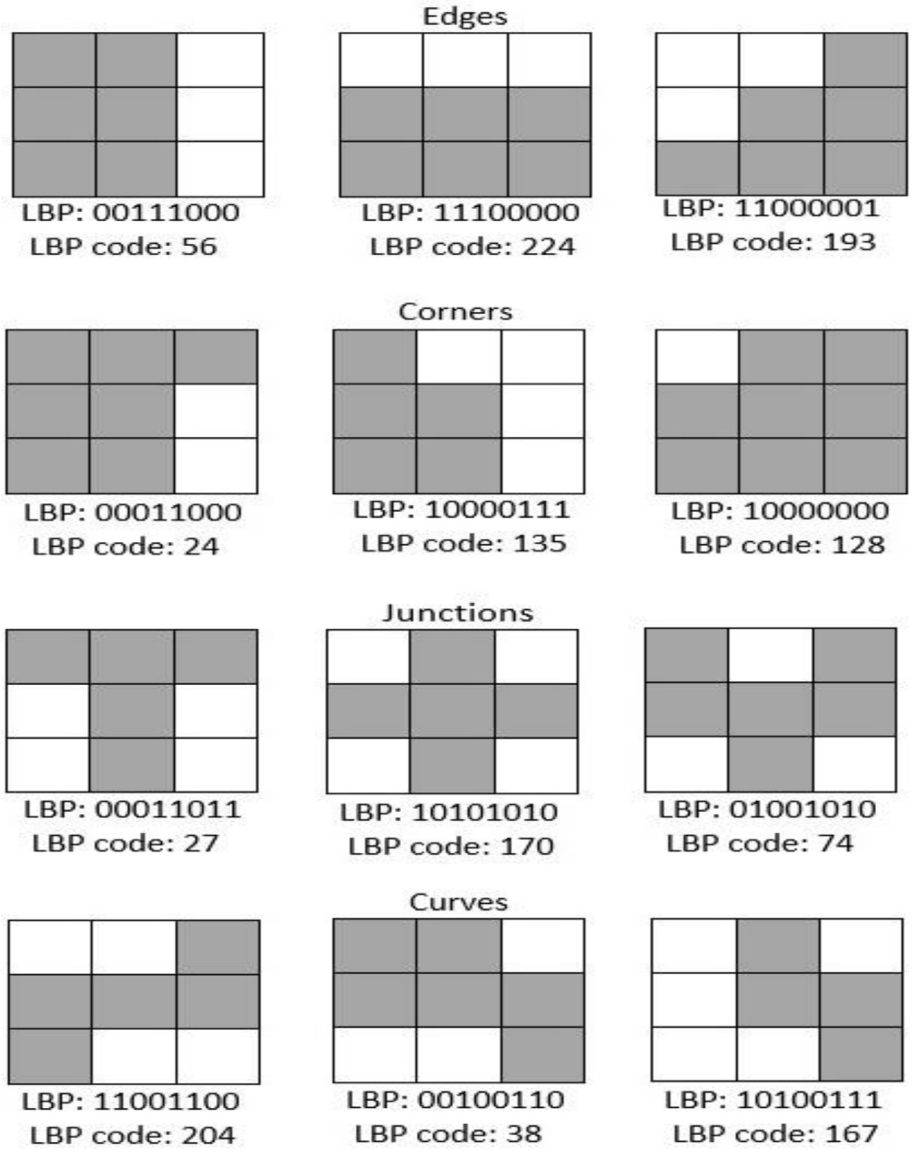

Fig. 7. Image Characteristic Model and their LBP codes.

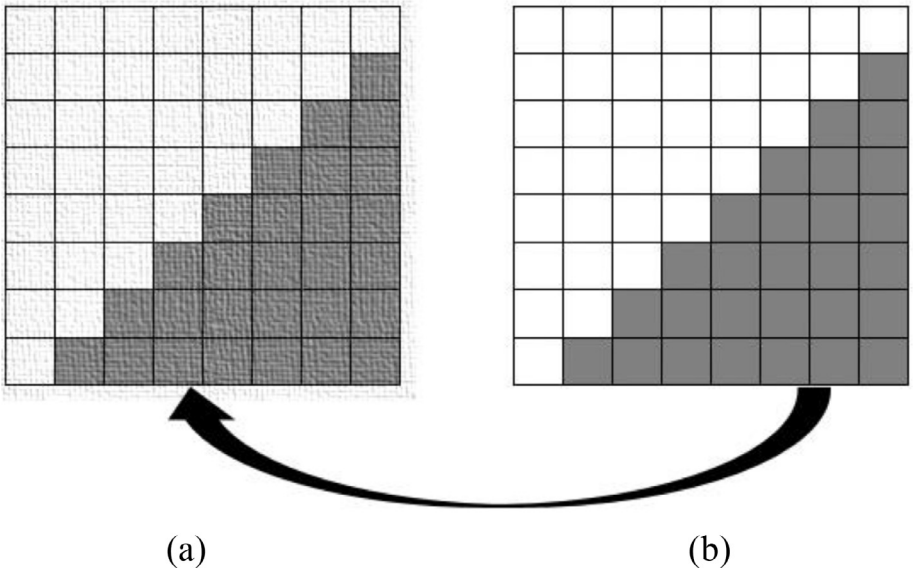

Fig. 8. DCT coefficient of a block of size 8 × 8 of the (a) resized test image (b) best matching HR training image. Unfilled pixels signify low-frequency coefficients. Filled pixels signify high-frequency coefficients.

the threshold value is decided and after that, the binary pattern is formed by thresholding the neighboring pixels. Then center pixel's value is revised as per binary pattern. Thus, the LBP code shows the fine details of the image in the given patch. The complete geometry of an image is recorded in the form of LBP codes by encoding the complete image with this proposed approach. LBP coding is done on the resized test image and LR images.

3.3. Searching for identical characteristic image

In this proposed approach, training LR images have minimum dissimilarity characteristics compared to test images. Here, LBP encoded test image and training LR image are converted in the patches of size 8×8. After that, each pixel in a patch of test image is compared with corresponding pixel of a patch of all training LR images. The LR image with a minimum absolute difference for the given patch is selected for optimum matching of patches. Thus, characteristic of the test image patch such as curves, corners and edges are matched maximum to the corresponding image patch of the searched training LR image.

Suppose, $\dot{P}_T(x,y)$ and $\dot{P}_{LRN}(x,y)$, be the test image patch of size 3×3 and N^{th} LR training image patch of size 3×3 respectively. $\breve{D}$ is an absolute error. Then, the nearest matching patch from the dataset can be minimizing error $\breve{D}$ using below equation (2):

$$\breve{D} = \sum_{x=1,y=1}^{8} \left[\left| \dot{P}_T(x,y) - \dot{P}_{LRN}(x,y) \right| \right] \tag{2}$$

This process is carried out on all the image patches of the test image and the optimum matched LR training images are searched corresponding to all test image patches.

3.4. Learning HR coefficients from HR image corresponds to best match LR image of database

Once optimum matched LR images are searched for all test images patches, high-resolution information is learned from the

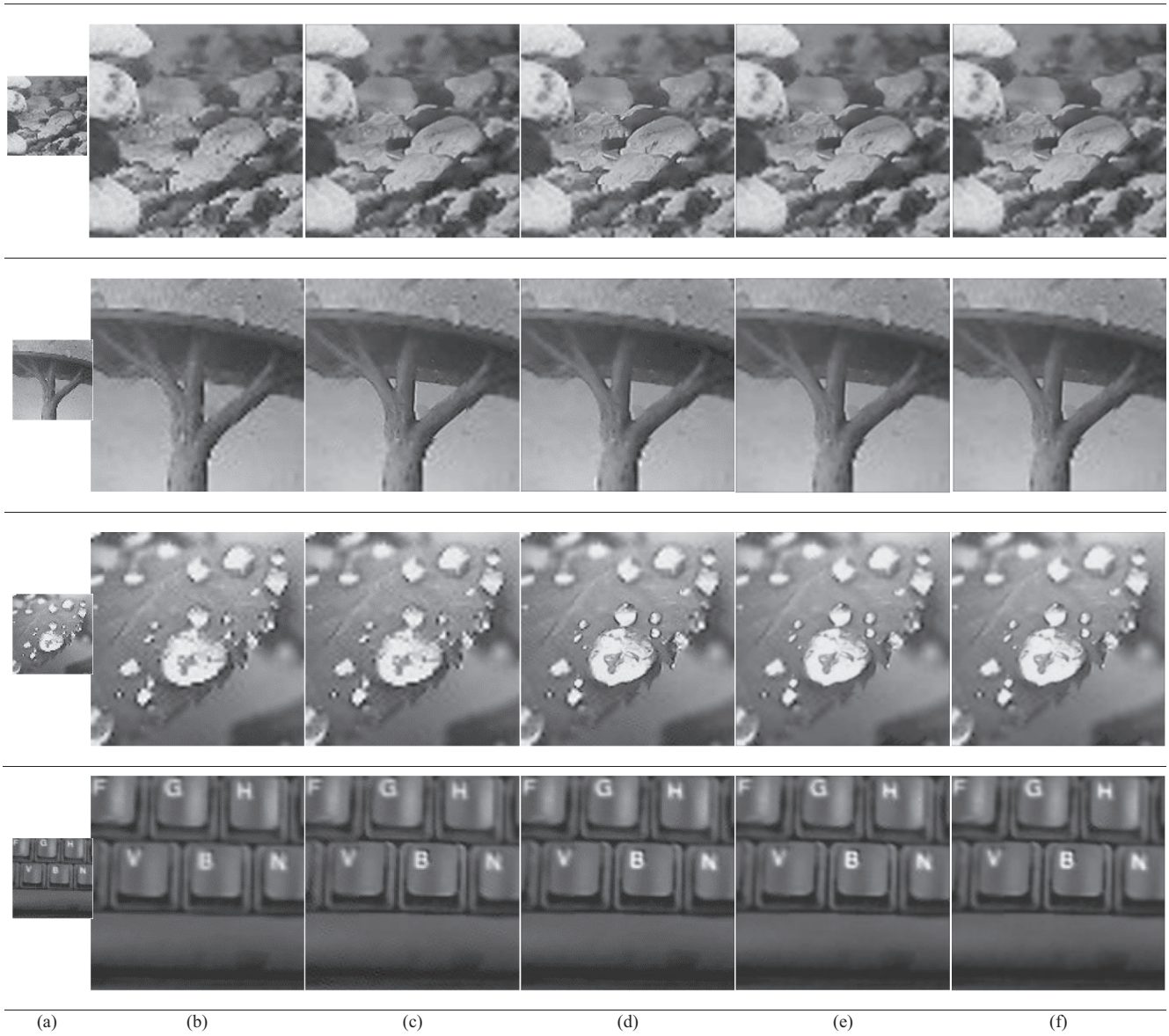

Fig. 9. (a) LR test image (b) Resultant HR image using Bicubic interpolation approach (c) Resultant HR image using Kalariya approach (Kalariya et al., 2015) (d) Resultant HR image using proposed approach with 8x8 DCT and LBP (e) Resultant HR image using proposed approach with 4×4 (f) Resultant HR image using proposed approach with 16×16 DCT and LBP.

corresponding HR training images. The resultant HR training images are true high-resolution images, then, high-frequency details in term of DCT coefficients are learned from the training HR images to enhance its resolution. Fig. 8 shows the learning procedure for HR coefficients. Here, high-frequency coefficients of 8×8 pixels block/patch of test image are learned from 8×8 pixels block/patch of the best-matched HR training image. The best-matched HR image is a high-resolution version of the optimum matched LR training image as defined in subsection 3.3.

The shaded boxes in Fig. 8 show HR coefficients of test image patch. These HR DCT coefficients are copied into the appropriate position of the test image patch. This task is repeated for all the 8×8 blocks of the test image. After completion of these learning process, inverse discrete cosine transform is applied to all patches of the test image to achieve final HR image.

4. Proposed approach for color images

In Section 3, steps of proposed approach for super-resolution of grayscale images are given. While in this section, modification of proposed approach for super-resolution of color images are described.

The existing correlations between color components in the resultant image are unbalanced by applying monochrome super-resolution technique to each of the R, G, and B color components. So that, the resultant super-resolute color image may have some artifacts. Also, computational load will be increased by applying super-resolution technique to all these components. To nullify these, color space transformation and separate the luminance and chrominance components are used in this approach for representation of the color images in YCbCr color space and expand them differently. The details of the luminance component are more important than that of chrominance components, as the sensitivity of the human eye is more to luminance component details. So that, the luminance component Y is super-resolute by proposed approach and enhancement in the chrominance components is done by the simple interpolation technique. The super-resolute color image is obtained by converting YCbCr to RGB color space using enhanced luminance and chrominance components.

5. Experimental results and discussion

In this section, the performance analysis and assessment of proposed approach are given. The real-world images are used to conduct all the experiments. The performance of proposed approach is also tested for remote sensing images which are described in Subsection 5.1. The performance of the proposed approach using DWT coefficients is given in Subsection 5.2.

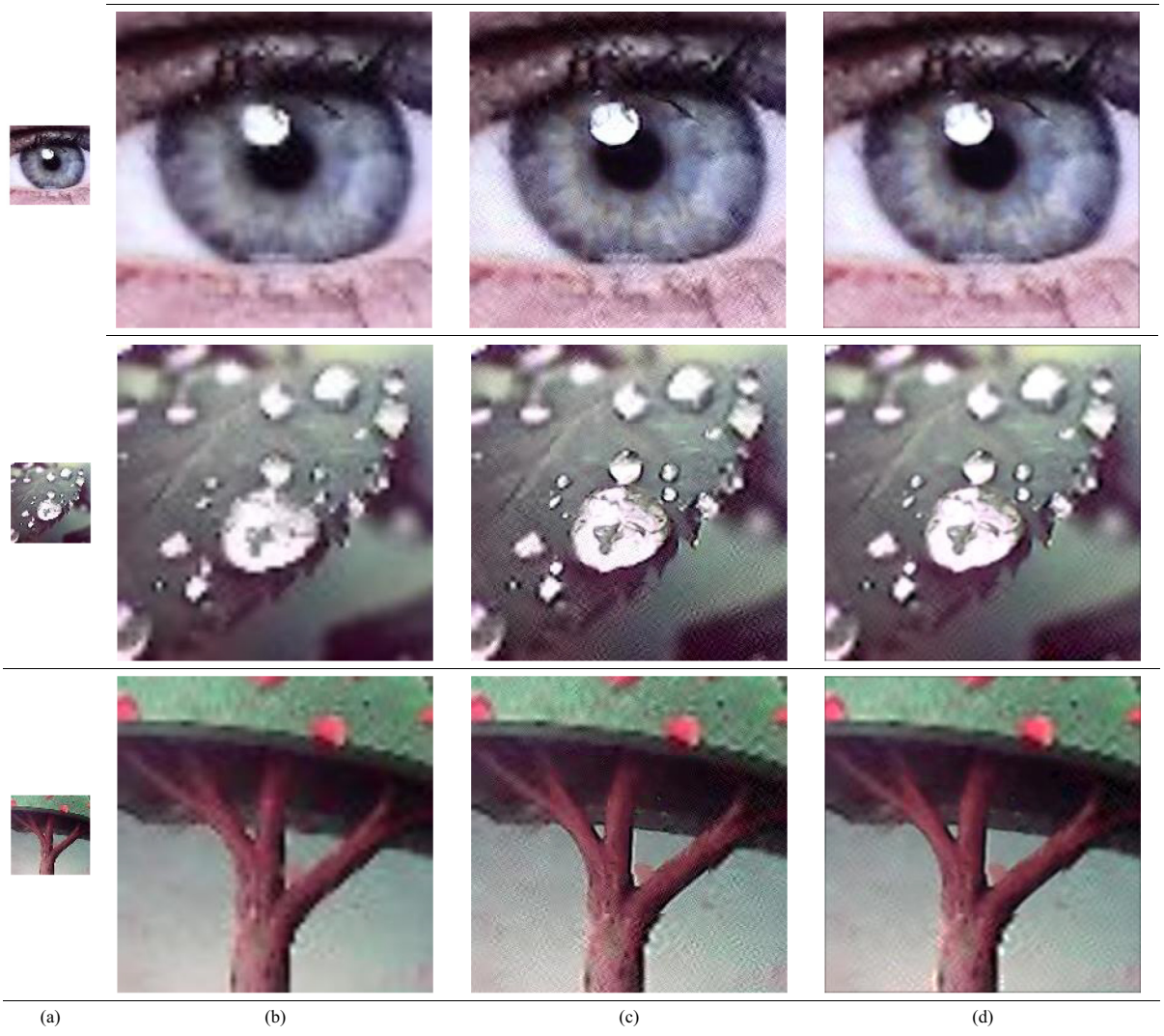

Fig. 10. (a) LR test color image of size 64×64 (b) Resultant HR color image using Bicubic interpolation approach (c) Resultant HR color image using Kalariya approach (Kalariya et al., 2015) (d) Resultant HR color image using proposed approach.

All recorded input images are captured at distinct zoom factors with the size of 64 × 64. The final SR image is of size 256 × 256. The training dataset contains almost 350 different sets of images. Each set of images consist of three images, an image with 1x zoom setting, 2× zoom setting and 4× zoom setting named as LR image-$S_1^{'}$, an HR image-$S_2^{'}$ and its HR image-$S_3^{'}$ respectively. To super-resolute$S_1^{'}$ image, LR-HR pair captured with 1-x and 2-x zoom are used. To super-resolute $S_2^{'}$ image, LR-HR pair captured with 2-x and 4-x zoom are used. Resolution technique used to obtain final SR image is based on DCT with LBP modelling.

From the dataset, some of the LR training images are taken as the test or observed images. Because of this, the true high-resolution versions of images are available for resultant parameter calculation. Here, LR and HR pairs of these observed images are removed from the dataset. Peak signal to noise ratio (PSNR), the Structural Similarity Index (SSIM), Mean Squared Error (MSE) and Mean Absolute Percentage Error (MAPE) (Wang et al., 2004; Wang and Bovik, 2009) values are calculated and compared with Bicubic interpolation and Kalariya approach (Kalariya et al., 2015) for qualitative and quantitative measurements. All the experiments are conducted on a computer with Intel Core i5-430IOM, 2.27 GHz processor and 4 GB RAM. The resultant test grayscale images and color images using proposed approach are given in Figs. 9 and 10, respectively. The subjective comparison of the proposed approach with Bicubic interpolation

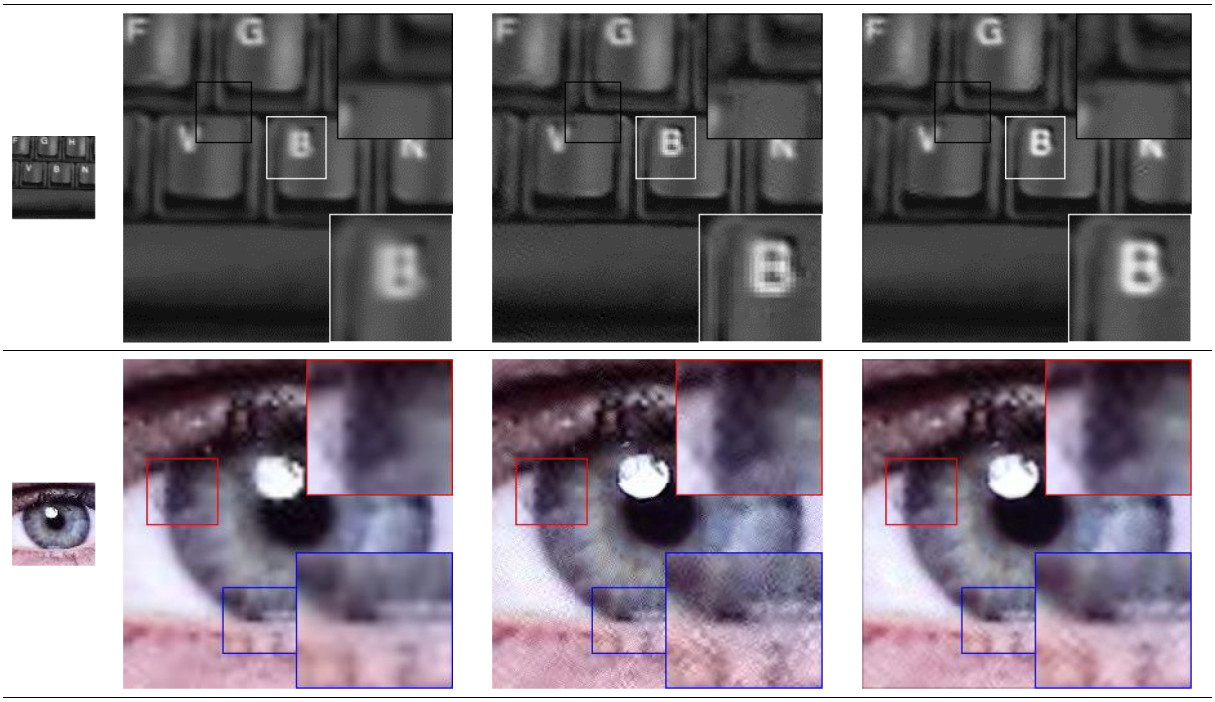

Fig. 11. Subjective comparison of the proposed approach with Bicubic Interpolation approach and Kalariya approach.

Table 1
Quality Parameters Values of Proposed Approach for Gray Scale Images.

Image	Bicubic Interpolation	Kalariya Approach (Kalariya et al., 2015)	Proposed approach with 4 × 4 DCT	Proposed approach with 8 × 8 DCT	Proposed approach with 16 × 16 DCT
PSNR (dB)					
STONE	31.6782	32.1965	35.5692	35.5155	35.4122
TREE	33.9675	34.6097	39.9624	40.3865	39.2459
LEAF	29.5416	30.1694	35.7230	34.1059	33.8533
KEYBOARD	34.7996	35.5290	40.9129	40.5770	40.9954
MSE					
STONE	44.1834	39.2130	18.0369	18.2614	18.8592
TREE	26.0812	22.4964	6.5590	5.9488	7.7355
LEAF	72.2638	62.5367	17.4092	25.2634	26.7762
KEYBOARD	21.5338	18.2044	5.2698	5.6935	5.1706
SSIM					
STONE	0.3851	0.4946	0.5087	0.5061	0.5092
TREE	0.6395	0.6880	0.7145	0.6937	0.7140
LEAF	0.5428	0.6378	0.6739	0.6854	0.6761
KEY BOARD	0.8545	0.8431	0.8692	0.8722	0.8709
MAPE					
STONE	16.8029	14.5279	11.0977	11.1023	11.1404
TREE	3.9855	3.0487	2.3849	2.5268	2.6720
LEAF	8.9203	6.5264	6.3690	6.4041	6.3889
KEY BOARD	3.7918	5.2551	2.2338	2.2552	2.2766

Table 2
Quality Parameters Values of Proposed Approach for Color Images.

Image	Bicubic Interpolation			Kalariya Approach (Kalariya et al., 2015)			Proposed approach with 8 × 8 DCT		
PSNR (dB)									
EYE	29.7907			30.0127			33.635		
LEAF	29.2149			29.2325			31.0503		
TREE	33.2265			31.9448			36.9569		
MSE									
EYE	68.2359			64.8349			28.1565		
LEAF	77.9094			77.5944			51.0561		
TREE	30.9338			41.5528			13.7213		
SSIM									
EYE	0.4711			0.4863			0.5941		
LEAF	0.5463			0.454			0.6016		
TREE	0.4194			0.4717			0.6228		
MAPE									
	R	G	B	R	G	B	R	G	B
EYE	22.4075	85.8109	13.2523	16.7938	80.5664	9.8038	13.2019	64.5157	1.0420
LEAF	21.2189	107.5928	21.4081	16.9388	102.4078	16.7740	13.4872	95.2194	16.0233
TREE	49.6231	122.1603	30.6091	46.1792	117.7200	27.0477	45.0028	83.8959	21.8216

Table 3
Comparison of Proposed Approach with Joshi Approach (Joshi et al., 2005).

Approach	Method employed	Approaches Used	PSNR (dB)
Joshi (Joshi et al., 2005)	Regularization based method	Use of either a Markov random field (MRF) or a simultaneous autoregressive (SAR) model to parameterize the field based	Between 22 and 26
Proposed	Example based/Learning based method	DCT with LBP as the characteristic model	Between 35 and 41

approach and Kalariya approach (Kalariya et al., 2015) is given in Fig. 11.

As shown in Fig. 9, it is found that in an image of STONE, there is an improvement in fine edges and texture details. While in an image of TREE chessboard effect is reduced enormously by the proposed approach. The outskirts fine details are recovered effectively in LEAF image. The better edges recovery and picture details are recovered immensely in KEYBOARD image using proposed approach. The quality measurement parameters of proposed approach are tabulated in Table 1. As seen in Table 1, the result of the 8 × 8 DCT with LBP is moderated over 4 × 4 and 16 × 16 DCT with LBP. Thus, it is preferred 8 × 8 DCT with LBP in the proposed approach. Tables 1 and 2 show the improvement in PSNR, MSE, SSIM, and MAPE for grayscale as well as color images. The results show that this proposed approach effectively works for every type of images.

Also, the results of proposed approach are compared with Joshi approach (Joshi et al., 2005); has employed a regularization-based image super resolution method form zoomed observation. The comparison of approaches is tabulated in Table 3. In Joshi approach, super-resolution problem is solved using the zoom as an effective cue by using a simple maximum a posteriori Markov random field (MAP-MRF) formulation and suitable regularization approaches. The parameters of the MRF and the simultaneous autoregressive (SAR) model, which model the high-resolution image, can be learned from zoomed observation. In this modelling of high resolution image either as a homogeneous MRF or a SAR model. Super resolution is done with zoom factor either $q = 2$ or $q = 4$. In these two cases, PSNR values of proposed approach are used for compression with PSNR values of Joshi approach (Joshi et al., 2005).

5.1. Performance analysis of proposed approach for remote sensing images

In this section, application of proposed approach for super-resolution of remote sensing images is given. The remote sensing images are taken from LANDSAT dataset (Satellite images, 2018). The resultant HR image using proposed approach is given in Fig. 12 and performance measurement parameters values are tabulated in Table 4. As seen in Table 4, it is indicated that this proposed approach effectively works for super-resolution of remote sensing images.

5.2. Performance analysis of proposed approach using DWT instead of DCT

In this section, analysis of the proposed approach using DWT is described. In this approach, the HR training images are fragmented into 1st level DWT. The final HR image is decomposed in the 1st level DWT and its vertical, horizontal and diagonal details are initialized with zero values. While A of final HR image (the sub-band 0) consists of sub-band 0 of resized image (2 M × 2 M) test image (M × M) as seen in Fig. 13.

Here, three images such as Least Zoom (LZ) image$S_1^{'}$, Zoom (Z) image $S_2^{'}$ and Most Zoom (MZ) image$S_3^{'}$ are used in the proposed approach. Just as DCT with LBP approach, in this approach, first $S_1^{'}$ image is magnified by a factor of four, which is LZ_Enhanced, denoted as an LZ_E image. Likewise, with the proposed SR technique, Z-$S_2^{'}$ image is magnified by a factor of two called Z_Enhanced image and denoted as a Z_E image. Training database consists of sets of three sized images. The size of LR images in the training database and test image are same whereas the size of HR images in a training database is one sized up as seen in Fig. 14.

The block diagram of proposed approach using DWT is given in Fig. 15. It consists of DWT of training HR images, image feature modelling with four neighborhood pixels, searching of matched LR image, and learning HR coefficients. As given in Fig. 16, four neighborhood pixel patch model is proposed to acquire the identical feature comparison between the training LR images and test LR images. Here, the minimum absolute error criterion is used for feature comparison. The j^{th} training LR image for which minimum absolute error is selected and HR coefficients are learned from

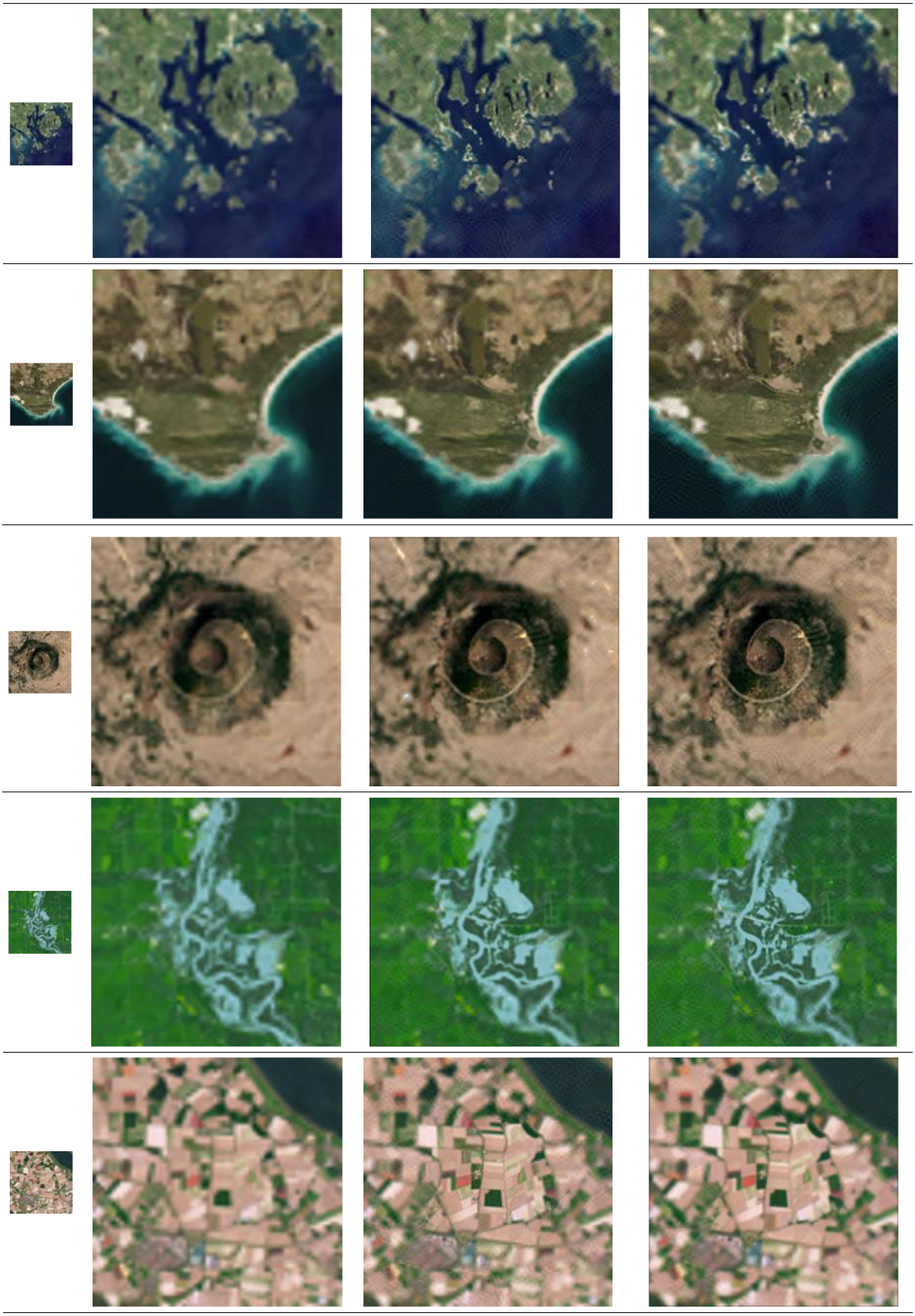

Fig. 12. (a) LR test color remote sensing image of size 64 × 64 (b) Resultant HR color remote sensing image using Bicubic interpolation approach (c) Resultant HR color remote sensing image using Kalariya approach (Kalariya et al., 2015) (d) Resultant HR color remote sensing image using proposed approach.

Table 4
Quality Parameters Values of Proposed Approach for Color Remote Sensing Images.

Image	Bicubic Interpolation			Kalariya Approach (Kalariya et al., 2015)			Proposed approach with 8 × 8 DCT with LBP		
PSNR (dB)									
Image 1	31.4821			32.5192			32.8591		
Image 2	33.2769			33.5889			35.0758		
Image 3	31.1827			31.1599			31.6153		
Image 4	30.7039			32.1809			33.0129		
Image 5	30.9772			31.4749			31.9044		
MSE									
Image 1	46.2241			36.4052			33.6644		
Image 2	30.5761			28.4569			20.207		
Image 3	49.7835			49.5234			44.8279		
Image 4	55.2947			39.3538			32.4933		
Image 5	51.9227			46.3005			41.9417		
SSIM									
Image 1	0.6799			0.7084			0.7261		
Image 2	0.7497			0.7621			0.7816		
Image 3	0.6097			0.6525			0.6689		
Image 4	0.6746			0.7144			0.7215		
Image 5	0.6899			0.7264			0.7363		
MAPE									
	R	G	B	R	G	B	R	G	B
Image 1	27.9236	17.2623	1.6113	24.7269	15.9058	1.5305	24.0967	15.7700	1.2665
Image 2	2.3727	0.7980	2.4643	3.5355	0.6622	2.0813	2.2324	0.6821	1.9897
Image 3	124.2950	24.7269	133.7524	92.7979	31.8726	144.5953	147.2900	21.3623	104.6814
Image 4	5.2063	0.3571	11.2076	3.9276	0.1541	9.8999	3.8208	0.2350	9.4727
Image 5	4.2847	2.9907	19.4733	4.8584	0.3281	2.5818	3.4012	0.2625	2.0813

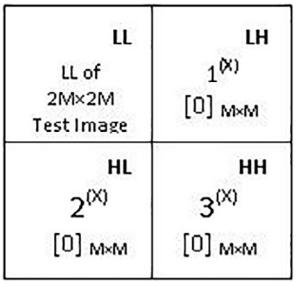

Fig. 13. Initialization of Final HR Image using 1st level DWT.

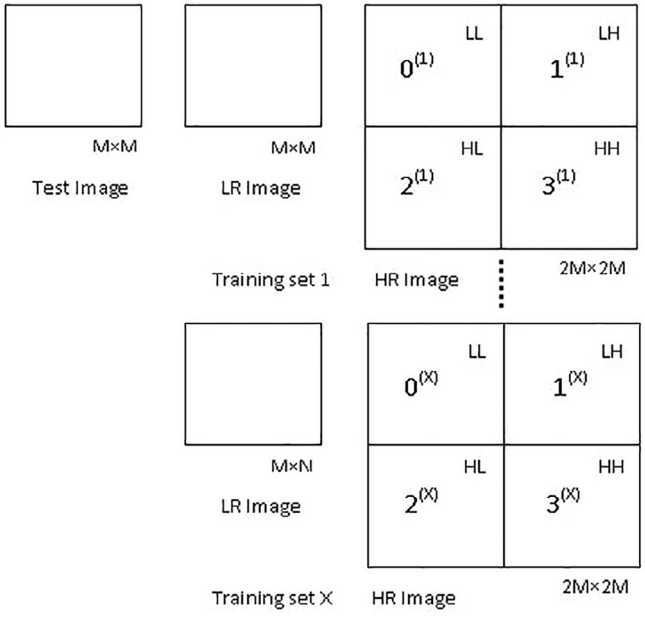

Fig. 14. An observed image of size M × M, Training dataset contains LR images of size M × M and HR images of size 2 M × 2 M.

corresponding j^{th} training HR image. Mathematically, this patch with size or 4 × 4 can be given using below equation (3):

$$I=\min_{1\leqslant j\leqslant n}\begin{bmatrix}|S(x,y)-T_j(x,y)|+|S(x+1,y)-T_j(x+1,y)|+\\ |S(x,y+1)-T_j(x,y+1)|+|S(x+1,y+1)-T_j(x+1,y+1)|\end{bmatrix} \tag{3}$$

Here, first, find finest matching LR image from the database using neighborhood pixels patch model. After getting the finest training LR image, the minimum absolute error is found for a patch of the observed image using learning of high resolution information in term of detail coefficients of DWT of corresponding training HR image. This learning process is given in Fig. 17.

Suppose the best match training LR image is T_j (size of M × M) for pixel (x,y) to test image S (size of M × M) under consideration. Let h_j (size of 2 M × 2 M) is corresponding HR image of the matched LR imageT_j. Wavelet coefficients$h_j(x,y+M)$, $h_j(x+M,y)$ and $h_j(x+M,y+M)$ are the wavelet coefficients corresponding to sub bands I, II and III respectively. Now sub bands of final HR image which are initialized with 'first' level DWT are replaced by the wavelet coefficients ofh_j. This is seen in the following equation (4):

$$\begin{aligned} FinalHR(x,y+M)&=h_j(x,y+M)\\ FinalHR(x+M,y)&=h_j(x+M,y)\\ FinalHR(x+M,y+M)&=h_j(x+M,y+M)\end{aligned} \tag{4}$$

Here, high frequency coefficients of the HR training image are placed into the final initialized HR image. After completion of this learning process inverse DWT of the learned image is performed to acquire resultant HR image.

The resultant images using a proposed approach based on DWT for grayscale images and color images are shown in Figs. 18 and 19, respectively. The quality values of this approach are tabulated in Table 5 and 6 for grayscale images and color images, respectively. The results in Tables 5 and 6 show that the proposed approach with 8x8 DCT with LBP is given better results compared to DWT based approach.

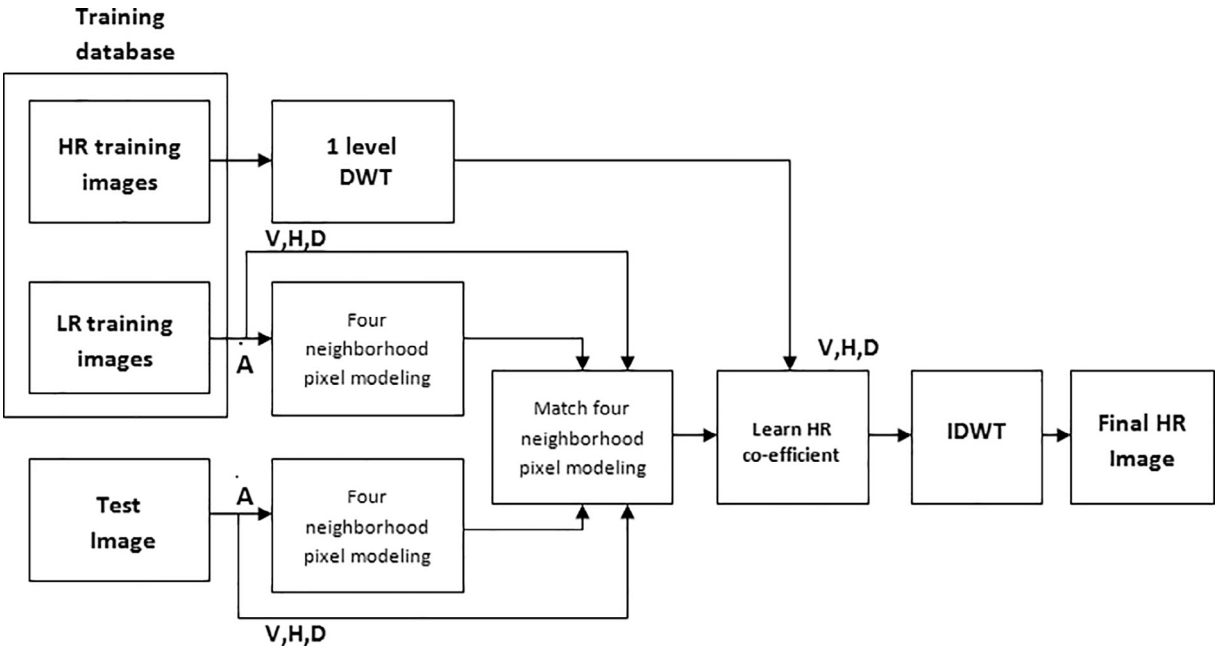

Fig. 15. Proposed Approach using DWT and LBP.

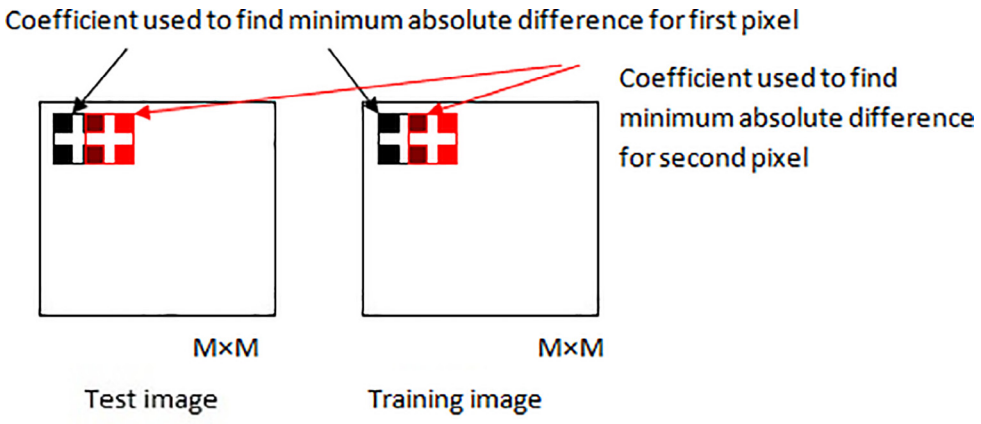

Fig. 16. Neighboring four pixels model for proposed approach.

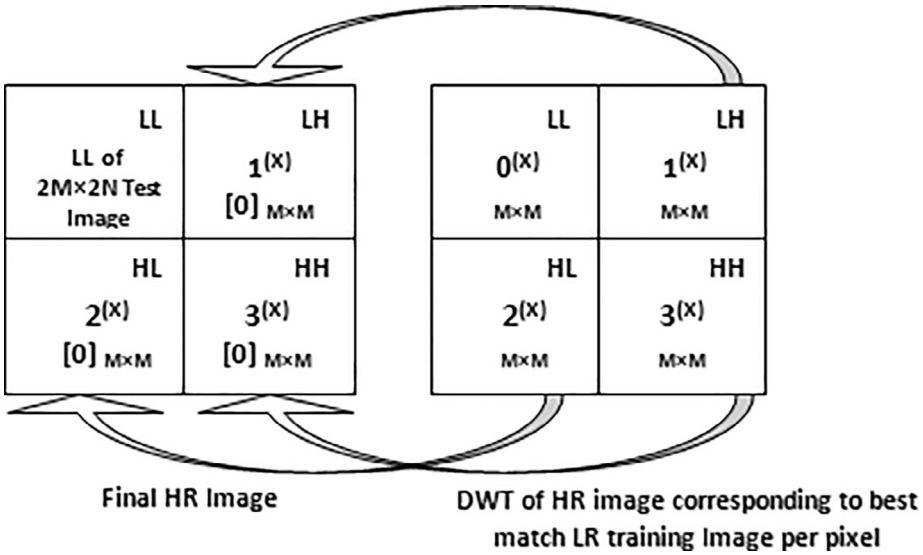

Fig. 17. Learning from LR-HR pair of training images using DWT.

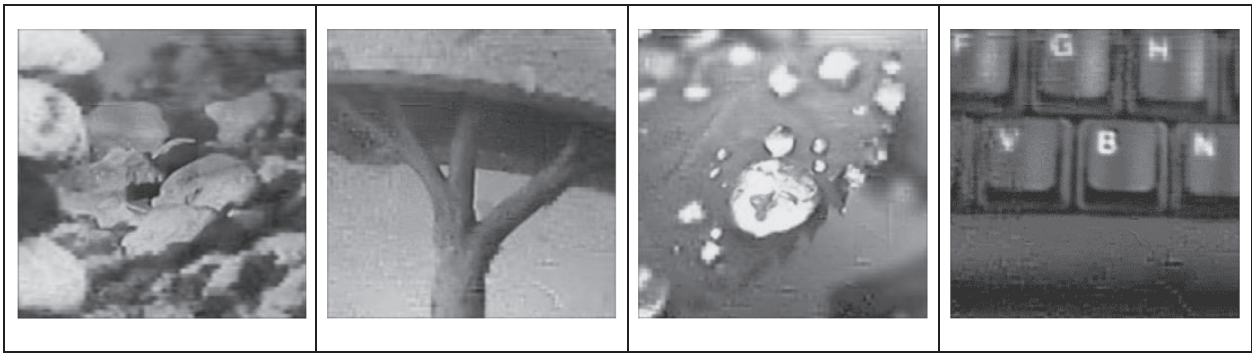

Fig. 18. Resultant HR grayscale images using proposed approach based on DWT.

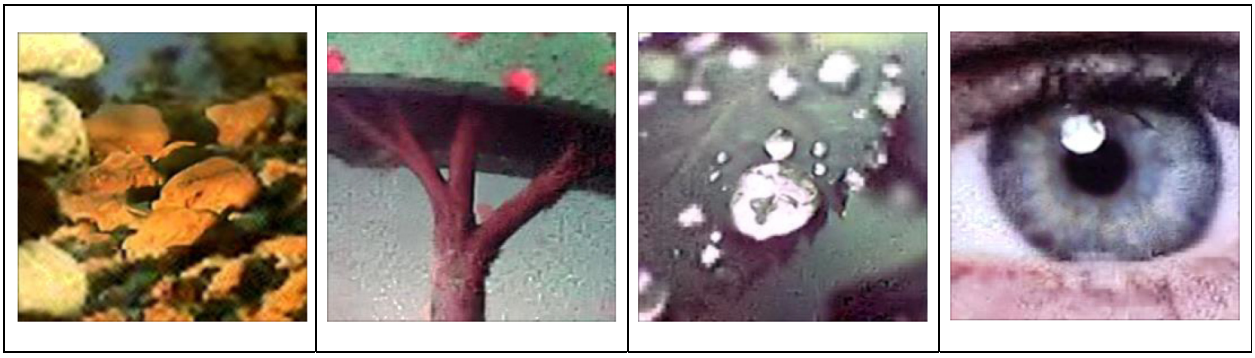

Fig. 19. Resultant HR color images using proposed approach based on DWT.

Table 5
Quality Parameters Values of Proposed Approach based on DWT for Grayscale Images.

Test Image	Proposed approach with DWT and four-pixel comparison model	Proposed approach with 8 × 8 DCT and LBP
PSNR (dB)		
STONE	35.1143	35.5155
TREE	38.5915	40.3865
ANIMAL	30.8129	29.3165
LEAF	31.9273	34.1059
ROSE	32.9179	36.2816
KEYBOARD	40.3049	40.5770
BOY FACE	41.3010	38.5753
MSE		
STONE	20.0286	18.2614
TREE	8.9935	5.9488
ANIMAL	52.8518	76.0554
LEAF	41.7206	25.2634
ROSE	33.2114	15.3078
KEYBOARD	6.0616	5.6935
BOY FACE	4.8193	9.0271
SSIM		
STONE	0.5065	0.5061
TREE	0.6534	0.6937
ANIMAL	0.5645	0.5659
LEAF	0.6469	0.6854
ROSE	0.6406	0.6452
KEYBOARD	0.7927	0.8722
BOY FACE	0.8297	0.9082

Table 6
Quality Parameters Values of Proposed Approach based on DWT for Color Images.

Test Image	Proposed approach with DWT and four-pixel comparison model	Proposed approach with DCT and LBP
PSNR (dB)		
STONE	34.7592	34.8570
TREE	36.8490	36.9569
BIRD	32.6780	33.4536
EYE	33.4506	33.6350
LEAF	30.2234	31.0503
ROSE	34.6604	35.2063
MSE		
STONE	21.7351	22.2526
TREE	13.4332	13.7213
BIRD	35.0980	29.3573
EYE	29.3780	28.1565
LEAF	61.7650	51.0561
ROSE	22.2352	19.6088
SSIM		
STONE	0.4305	0.4392
TREE	0.5447	0.6228
BIRD	0.5995	0.6037
EYE	0.5587	0.5941
LEAF	0.5771	0.6016
ROSE	0.5667	0.5846

6. Conclusions

In this paper, a new super-resolution approach based on various image transform such as DCT, DWT, and LBP model is proposed for the image. In this approach, three images are acquired with distinct zoom factors of the same static scene for analysis. The experimental results show that this proposed approach is effectively worked on various types of natural images such as grayscale image and color image. Also, the performance of this proposed approach is compared with two existing approaches such as Kalariya et al., 2015 and Joshi et al. (2005). The comparison of approaches shows that the performance of proposed approach is better than existing approaches. This proposed approach can be useful in the analysis of scene of a specific region of the image in various applications such as wildlife photography, satellite imaging system, etc. In near future, the performance of this approach will be tested using advance image transform such as curvelet and contourlet.

References

Tian, J., Ma, K.K., 2011. A survey on super-resolution imaging. SIViP 5 (3), 329–342.

Park, S.C., Park, M.K., Kang, M.G., 2003. Super-resolution image reconstruction: a technical overview. IEEE Signal Process Mag. 20 (3), 21–36.

Ji, H., Fermüller, C., 2009. Robust wavelet-based super-resolution reconstruction: theory and algorithm. IEEE Trans. Pattern Anal. Mach. Intell. 31 (4), 649–660.

Chappalli, M.B., Bose, N.K., 2005. Simultaneous noise filtering and super-resolution with second-generation wavelets. IEEE Signal Process Lett. 12 (11), 772–775.

El-Khamy, S.E., Hadhoud, M.M., Dessouky, M.I., Salam, B.M., El-Samie, F.E.A., 2005. Regularized super-resolution reconstruction of images using wavelet fusion. Opt. Eng. 44, (9) 097001.

Aftab, H., Mansoor, A.B., Asim, M., 2008, December. A new single image interpolation technique for super-resolution. In: Multitopic Conference, 2008. INMIC 2008. IEEE International (pp. 592–596). IEEE.

Suresh, K.V., Rajagopalan, A.N., 2007. Robust and computationally efficient super resolution algorithm. JOSA A 24 (4), 984–992.

Belekos, S.P., Galatsanos, N.P., Katsaggelos, A.K., 2010. Maximum a posteriori video super-resolution using a new multichannel image prior. IEEE Trans. Image Process. 19 (6), 1451–1464.

Shen, H., Zhang, L., Huang, B., Li, P., 2007. A MAP approach for joint motion estimation, segmentation, and super-resolution. IEEE Trans. Image Process. 16 (2), 479–490.

Jung, C., Ju, J., 2013, May. Improving dictionary based image super-resolution with nonlocal total variation regularization. In: Circuits and Systems (ISCAS), 2013 IEEE International Symposium on (pp. 1207–1211). IEEE.

Zibetti, M.V., Bazán, F.S., Mayer, J., 2011. Estimation of the parameters in regularized simultaneous super-resolution. Pattern Recogn. Lett. 32 (1), 69–78.

Vicente, A.N., Pedrini, H., 2016, October. A learning-based single-image super-resolution method for very low-quality license plate images. In: Systems, Man, and Cybernetics (SMC), 2016 IEEE International Conference on (pp. 000515-000520). IEEE.

Hertzmann, A., Jacobs, C. E., Oliver, N., Curless, B., Salesin, D.H., 2001, August. Image analogies. In: Proceedings of the 28th annual conference on Computer graphics and interactive techniques (pp. 327–340). ACM.

Wang, J., Zhu, S., Gong, Y., 2010. Resolution enhancement based on learning the sparse association of image patches. Pattern Recogn. Lett. 31 (1), 1–10.

Kim, K.I., Kwon, Y., 2010. Single-image super-resolution using sparse regression and natural image prior. IEEE Trans. Pattern Anal. Mach. Intell. 32 (6), 1127–1133.

Mu, G., Gao, X., Zhang, K., Li, X., Tao, D., 2011, September. Single image super resolution with high resolution dictionary. In: Image Processing (ICIP), 2011 18th IEEE International Conference on (pp. 1141–1144). IEEE

Kim, K.I., Kwon, Y., 2008. June). Example-based learning for single-image super-resolution. In: Joint Pattern Recognition Symposium. Springer, Berlin, Heidelberg, pp. 456–465.

Rhee, S., Kang, M.G., 1999. Discrete cosine transform based regularized high-resolution image reconstruction algorithm. Opt. Eng. 38 (8), 1348–1357.

Parmar, H.M., Scholar, P.G., 2014. Comparison of DCT and wavelet based image compression techniques. Int. J. Eng. Dev. Res. 2, 664–669.

Dabbaghchian, S., Ghaemmaghami, M.P., Aghagolzadeh, A., 2010. Feature extraction using discrete cosine transform and discrimination power analysis with a face recognition technology. Pattern Recogn. 43 (4), 1431–1440.

Gajjar, P.P., Joshi, M.V., 2008, December. Single frame super-resolution: a new learning based approach and use of IGMRF prior. In: Computer Vision, Graphics & Image Processing, 2008. ICVGIP'08. Sixth Indian Conference (pp. 636–643). IEEE.

Pithadia, P.V., Gajjar, P.P., Dave, J.V., 2012, July. Super-resolution using DCT based learning with LBP as feature model. In: Computing Communication & Networking Technologies (ICCCNT), 2012 Third International Conference on (pp. 1–6). IEEE.

Kalariya, P.G., Gajjar, P.P., Muliya, P.J., 2015. DCT based Learning Approach for Image Super-Resolution from Zoomed Observations. In: National Conference on Digital Image and Signal Processing, DISP 2015 (pp. 7–11).

Ahonen, T., Hadid, A., Pietikainen, M., 2006. Face description with local binary patterns: Application to face recognition. IEEE Trans. Pattern Anal. Mach. Intell. 28 (12), 2037–2041.

Pereira, E.T., Gomes, H.M., De Carvalho, J.M., 2010, August. Integral local binary patterns: a novel approach suitable for texture-based object detection tasks. In: Graphics, Patterns and Images (SIBGRAPI), 2010 23rd SIBGRAPI Conference on (pp. 201–208). IEEE.

Ojala, T., Pietikainen, M., Maenpaa, T., 2002. Multiresolution gray-scale and rotation invariant texture classification with local binary patterns. IEEE Trans. Pattern Anal. Mach. Intell. 24 (7), 971–987.

Gajjar, P., Joshi, M., 2010, June. Zoom based super-resolution: A fast approach using particle swarm optimization. In: International Conference on Image and Signal Processing (pp. 63–70). Springer, Berlin, Heidelberg.

Gajjar, P.P., Joshi, M.V., Banerjee, A., Mitra, S., 2006. Decimation estimation and super-resolution using zoomed observations. In: Computer Vision, Graphics and Image Processing (pp. 45–57). Springer, Berlin, Heidelberg.

Joshi, M.V., Chaudhuri, S., Panuganti, R., 2005. A learning-based method for image super-resolution from zoomed observations. IEEE Trans. Syst. Man Cybern. Part B (Cybernetics) 35 (3), 527–537.

Wang, Z., Bovik, A.C., Sheikh, H.R., Simoncelli, E.P., 2004. Image quality assessment: from error visibility to structural similarity. IEEE Trans. Image Process. 13 (4), 600–612.

Wang, Z., Bovik, A.C., 2009. Mean squared error: Love it or leave it? A new look at signal fidelity measures. IEEE Signal Process Mag. 26 (1), 98–117.

Satellite images from link https://landsat.visibleearth.nasa.go last access on May 2018.